Photodiagnosis and Photodynamic Therapy 25 (2019) 369–375

Contents lists available at ScienceDirect

Photodiagnosis and Photodynamic Therapy

journal homepage: www.elsevier.com/locate/pdpdt

Application of different noninvasive diagnostic techniques used in HMME-PDT in the treatment of port wine stains

Long Wen[a,1], Yunfeng Zhang[b,1], Linglin Zhang[b], Xiaojing Liu[b], Peiru Wang[b], Shuzhan Shen[b], Chan Hu[b], Lehang Guo[c], Wencai Jiang[d], Ronald Sroka[b,e], Xiuli Wang[a,b,*]

[a] Shanghai Skin Disease Clinical College of Anhui Medical University, Shanghai Skin Disease Hospital, China
[b] Institute of Photomedicine, Shanghai Skin Disease Hospital, Tongji University School of Medicine, Shanghai, China
[c] Department of Medical Ultrasound, Shanghai Tenth People's Hospital, Ultrasound Research and Education Institute, Tongji University School of Medicine, Shanghai, China
[d] Department of Skin and Cosmetic Research, Shanghai Skin Disease Hospital, Shanghai, China
[e] Laser-Forschungslabor, LIFE-Center of University Hospital of LMU, Department of Urology, University of LMU, Munich, Germany

ARTICLE INFO

Keywords:
Port-wine stains
Hematoporphyrin monomethyl ether photodynamic therapy
VISIA-CR™ system
Dermoscopy
High-frequency ultrasound
Laser speckle contrast imaging

ABSTRACT

Background: Hematoporphyrin monomethyl ether photodynamic therapy (HMME-PDT) is an effective method for treating port wine stains (PWS). However, methods to evaluate the treatment of HMME-PDT for PWS effectively and objectively are lacking.

Objective: This study aimed to describe the different noninvasive diagnostic techniques used in the evaluation of treatment response to HMME-PDT for PWS.

Methods: Thirty-one lesions of 22 patients with PWS were treated with HMME-PDT. Four noninvasive diagnostic techniques including VISIA-CR™ system, dermoscopy, high-frequency ultrasound (HFUS), and laser speckle contrast imaging (LSCI) were used to obtain standard radiographic data on skin color, skin thickness, blood vessel morphology, blood vessel distribution, and blood perfusion from lesions and surrounding normal skin before and after HMME-PDT.

Results: The standard image pattern of VISIA-CR™ system showed color change in the lesions of PWS after HMME-PDT. RBX red image of VISIA-CR™ system showed that erythema was highly aggregated even in invisible lesions at baseline but decreased after HMME-PDT. The erythema index reduced value *d* was related to the efficacy rating ($\gamma = 0.631$, $P < 0.05$). Dermoscopy showed that the number of spot-like and irregular linear vessels increased, which was correlated with the increase in clinical classification. After HMME-PDT, vascular rupture was observed by dermoscopy. The response rate of lesions with vascular rupture was 100.00% (20/20). Moreover, the response rate of lesions without vascular rupture was 63.64% (7/11). Vascular rupture sign was correlated with better efficacy ($P < 0.05$). HFUS showed that the dermis of PWS thickened and was arranged loosely with scattered linear hypoechoic signal. After HMME-PDT, the dermal layer of the lesions became thinner with a decreased linear hypoechoic signal. The response rate of the lesions with linear hypoechoic signal was 76.92% (10/13), and that without linear hypoechoic signal was 94.44% (17/18). The lesions without linear hypoechoic signal in the dermis showed better efficacy ($P < 0.05$). In some lesions, LSCI showed high blood perfusion signal in PWS lesions and blood perfusion reduction after HMME-PDT.

Conclusion: VISIA-CR™ system can be used to observe not only visible but also invisible lesions of PWS. Moreover, lesions fading after HMME-PDT can be described objectively by VISIA-CR™ system. Dermoscopy played an important role in the clinical classification of PWS, including assessing vascular injury after HMME-PDT, guiding the adjustment of therapeutic dose, and selecting the end point of treatment. Both HFUS and LSCI can be used to assist treatment response evaluation of HMME-PDT.

* Corresponding author at: Institute of Photomedicine, Shanghai Skin Disease Hospital, Tongji University School of Medicine, 1278 Baode Road, Shanghai, 200443, China.
E-mail address: wangxiuli_1400023@tongji.edu.cn (X. Wang).
[1] co-first author.

https://doi.org/10.1016/j.pdpdt.2019.01.008
Received 16 July 2018; Received in revised form 27 November 2018; Accepted 4 January 2019
Available online 06 January 2019

1. Introduction

Port wine stain (PWS) is a type of congenital, low blood flow skin vascular malformation generally located on the face and neck [1]. The prevalence of PWS in neonates is 0.3%–0.5%, and it cannot be usually resolved by self-healing. The color and thickness of lesions will progress with age, and some of them may develop to nodules [2].

Hematoporphyrin monomethyl ether photodynamic therapy (HMME-PDT) has been proved as an effective new method for the treatment of PWS in recent years with its unique advantages of being safe, non-invasive, and highly selective for blood vessels, which can be used to treat large skin lesions [3]. At present, the evaluation of the clinical efficacy of the treatment for PWS is mainly based on subjective evaluations performed by the clinician with naked eyes. However, sometimes, small changes are difficult to detect. Histopathology is always considered the gold standard but is invasive and accompanied by pain inevitably. Therefore, some noninvasive, efficient, and accurate evaluation methods are needed. In recent years, noninvasive diagnostic techniques have been attempted in skin detection such as VISIA-CR™ system, dermoscopy, high-frequency ultrasound (HFUS), and laser speckle contrast imaging (LSCI), which may be useful in future for noninvasive detection of PWS in HMME-PDT.

VISIA-CR™ system image acquisition was operated by white and cross-polarized light, the latter of which is used to produce the RBX red image. Canfield's patented RBX™ (Red/Brown/X) [4] technology provides a semiquantitative assessment of specific chromophores in the skin [5]. Specifically, it measures the amount of hemoglobin content. Hemoglobin serves as a measure of the amount of redness in the skin, including those in background erythema, telangiectasias, and vascular lesions.

Dermoscopy is a noninvasive microscopic image analysis technique with polarized light. Skin structure such as epidermis, dermal papilla, and dermis and pigment of the skin can be observed by dermoscopy in vivo [6]. In clinical practice, dermoscopy can help improve the diagnostic accuracy of pigmented dermatosis [7], especially for early diagnosis of malignant melanoma [8].

Since Alexander and Miller began to discuss the application of HFUS in the research of skin diseases in 1979 [9], HFUS has made considerable progress recently. HFUS is a technique that uses variable frequencies to determine skin characteristics. It can clearly define the skin layer and deeper structure and provide a real-time local perfusion mode. A large number of studies showed that frequencies of HFUS above 15 MHz could provide meaningful diagnostic information for skin diseases. HFUS has been used for the detection of characteristic changes in a variety of dermatological diseases (superficial skin tumors, bacterial infectious skin diseases, connective tissue diseases, erythematous scaly skin diseases, dermatitis, and eczema) [10,11].

LSCI is a noncontact near-infrared imaging system with high temporal and spatial resolution to detect surface blood flow [12]. LSCI forms a full-field perfusion map of the detection area through real-time blood flow detection based on speckle contrast analysis. Currently, LSCI has been successfully used to measure blood perfusion in the cerebral cortex, liver, renal cortex, and gastric microvessels [13–17].

In this study, VISIA-CR™ system, dermoscopy, HFUS, and LSCI were used to evaluate the treatment response of HMME-PDT for PWS.

2. Methods

2.1. General information

The study included 22 outpatients (10 men and 12 women) with 31 lesions of PWS treated in Shanghai Skin Disease Hospital between March 2017 and January 2018. They were aged between 3 and 39 years. All lesions were located on the face and neck. Among all lesions, 8 lesions were pink type, 21 were purple type, and 2 were thickening type.

According to the requirements of medical ethics, all patients, and guardians of patients below 18 years of age, were informed of the purpose of the study. Then, the operation procedures and risks were explained to them. The patient signed the informed consent form for data collection.

2.2. HMME-PDT treatment

Hematoporphyrin monomethyl ether (5 mg/kg) was injected intravenously according to body weight. Ten minutes after injection, the lesion was irradiated by 532-nm LED light (spot size, 10 cm × 10 cm; power density, 80–100 mW/cm^2; treatment time, 20–30 min) [18]. Hemoporfin and 532-nm LED light were from Shanghai Fudan-Zhangjiang Bio-pharmaceutical Co., Ltd., China.

2.3. Efficacy evaluation

Eight weeks after HMME-PDT, four evaluators independently graded the improvement of PWS according to color blanching of baseline in the treated area using the following standard: ① cured, color of the lesion almost completely regressed (degree of improvement ≥90%); ② good effect, color of the lesion subsided significantly (degree of improvement ≥60%, < 90%); ③ alleviation, color of the lesion partially subsided (degree of improvement ≥20%, < 60%); ④ no effect, color was mostly unchanged in the treated area (degree of improvement < 20%) [3]. Those rated as cured, good effect, and alleviation were classified as the effective group, and those with no effect were classified as the ineffective group. The standard of efficacy evaluation through VISIA-CR™ system RBX red image was the same as above.

2.4. Noninvasive assessment

During HMME-PDT and follow-up, four non-invasive diagnostic techniques were used to record and analyze lesions as shown in Fig. 1:

1) VISIA-CR™ system (Canfield, USA; including 6500-K standard white

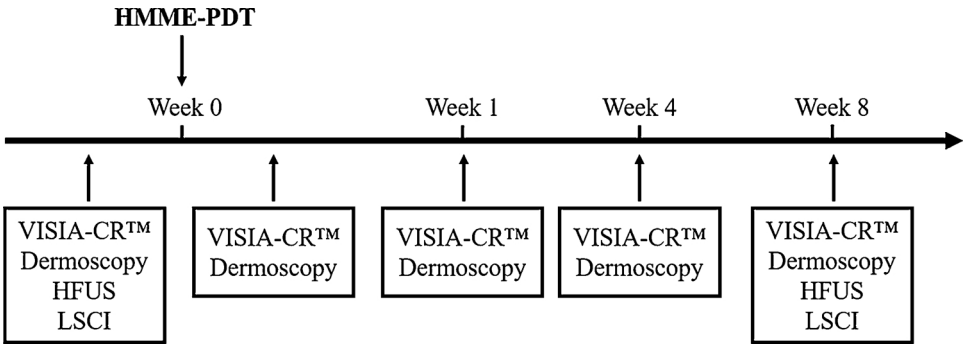

Fig. 1. Non-invasive diagnostic techniques detection timeline.

light and polarized light source): after the face of patient was cleaned, the chin was placed on a support cushion with the forehead close to the upper cushion, and then, the frontal and lateral images were taken in the darkroom with eyes closed.
2) Dermoscopy (MoleMax HD, Derma Medical Systems Handels-und Entwicklungs GmbH, Vienna, Austria; polarized light source, ×30-×100 magnification): dermoscopy was used in the skin directly with appropriate pressure to obtain images (×30).
3) HFUS (MD-300S HFUS, MEDA Co., Ltd., Tianjin, China; ultrasound frequency is 50 MHz; resolution is 50 μm): HFUS was used to measure the lesion with optimal pressure.
4) LSCI (MoorFLPI, Moor Instruments Ltd., Axminster, UK): blood perfusion in the lesion area is detected with MoorFLPI.

Each noninvasive measurement was used by the same clinician in the same environment. All data and images were archived.

2.5. Statistical method

Comparisons of baseline characteristics and occurrence rate of treatment reactions between the effective and ineffective groups were performed by chi-square test. We defined the correlation coefficient γ by nonparametric Spearman correlation test. All statistical tests had a two-sided significance level of < 0.05. SPSS 22.0 software was used for all data analyses.

3. Results

3.1. Treatment efficacy

After HMME-PDT, two of the 31 lesions of PWS were cured (6.45%), six lesions showed good effect (19.35%), 19 lesions showed alleviation (61.29%), and four lesions showed no effect (12.90%). The overall response rate was 87.10%.

3.2. Results of the VISIA-CR™ system

VISIA-CR™ system standard image showed the color fading before and after treatment of the lesion intuitively. RBX red image showed highly aggregated and densely distributed blood vessels in the lesion of patients with PWS. Moreover, inconspicuous lesions could be observed in the RBX red image. The color of the lesion is deepened within one week after PDT. Subsequently, the color of the erythema subsided gradually (Fig. 2). The erythema index reduced value *d* was correlated to the efficacy rating ($\gamma = 0.631$, $P < 0.05$). The efficacy evaluation through the VISIA-CR™ system RBX red image showed different response rates. Two of the 31 lesions of PWS were treated (6.45%), seven lesions showed good effect (22.58%), 19 lesions showed alleviation (61.29%), and three lesions showed no effect (9.67%). The overall response rate was 90.32%.

3.3. Results of dermoscopy

As shown in Fig. 3, different types of PWS showed different manifestations under dermoscopy: the pink type showed irregular linear and spot-like blood vessels on a bright red background; the purple type showed a densely distributed spherical blood vessel on the deep red background; the thickened type showed lump-like blood vessels on the magenta background. After HMME-PDT, vascular rupture was observed under the microscope in 20 lesions (Fig. 3). The response rate of lesions with vascular rupture was 100% (20/20). Moreover, the response rate of lesions without vascular rupture was 63.64% (7/11). After HMME-PDT, lesions with vascular rupture showed better efficacy ($P < 0.05$).

3.4. Results of HFUS

HFUS showed thicker lesions than the normal skin, and the dermis was arranged loosely (Fig. 4). The dermis of 13 lesions showed scattered linear hypoechoic signal. The response rate of lesions with linear hypoechoic signal was 76.92% (10/13). Moreover, the response rate of lesions without linear hypoechoic signal was 94.44% (17/18). The lesions without linear hypoechoic signal in the dermis showed better efficacy ($P < 0.05$). After HMME-PDT, the thickened dermis became thinner significantly, and linear hypoechoic signal also reduced significantly. Furthermore, the dermis was denser than that before therapy (Fig. 4).

3.5. Results of LSCI

In patients with PWS, the lesions showed rich blood perfusion signal using real-time LSCI. After HMME-PDT, the blood perfusion signal was reduced in 17 lesions (Fig. 5). Of the effective lesions, 87.72% (17/27) showed blood perfusion signal reduction, while 12.28% (10/27) showed no reduction. There was no blood perfusion signal reduction in the ineffective group.

4. Discussion

PWS is the most common type of congenital venous malformation. According to its clinical manifestations, it can be divided into three types: pink, purple, and thickened types [19]. Histopathology showed that the diameter of the blood vessels was about 10–300 um and the depth was about 100–1000 um. There was no obvious abnormality in the epidermis. The capillaries expanded with age, which can extend to the subdermal tissues [20].

Previously, pulsed dye laser (PDL) was the preferred treatment for PWS [21]. However, only lesions with a blood vessel diameter of 50–150 μm can be effectively treated with PDL. Simultaneously, age, lesion depth, and lesion extent also have a great impact on the response on PDL. Therefore, the clinical cure rate was not high. Recently, HMME-PDT has been developed as vascular-targeted photodynamic therapy for PWS [22]. Because of its advantages of targeting vessels, being noninvasive, and having large-area treatment, it has been widely used in clinical practice [23].

The evaluation of therapeutic efficacy of PWS had always depended on the subjective evaluation of physicians, which lacks objectivity. With the development of noninvasive diagnostic techniques, new skin imaging techniques are being used in the diagnosis and treatment of skin diseases such as VISIA-CR™ system, dermoscopy, HFUS, and LSCI [24]. In view of the difficulties in making an objective assessment, the above four noninvasive diagnostic techniques were used to analyze the efficacy of HMME-PDT in order to obtain a preliminary evaluation of the effect.

4.1. The application value of the VISIA-CR™ system

The standard images collected under the 6500-K white light were comparable before and after HMME-PDT. The RBX red image can show the distribution of superficial blood vessels in the skin. Micali et al. used RBX red image in the study of erythema, telangiectasia, and rosacea [25]. They found that this model can be used in the preliminary assessment of vascular components in the erythema area. This may help in the selection of the best treatment strategy. Our results revealed that lesions in patients with PWS showed more abundant vascular aggregation than the normal skin in RBX red image. Simultaneously, the abnormal capillary network that was not easily observed by the naked eye could be observed in the RBX red image. It was meaningful in the determination of the boundary of the lesion and precise treatment. Immediately after HMME-PDT, red deepening of the skin lesions could be observed in the RBX red image. This was caused by the rupture of the

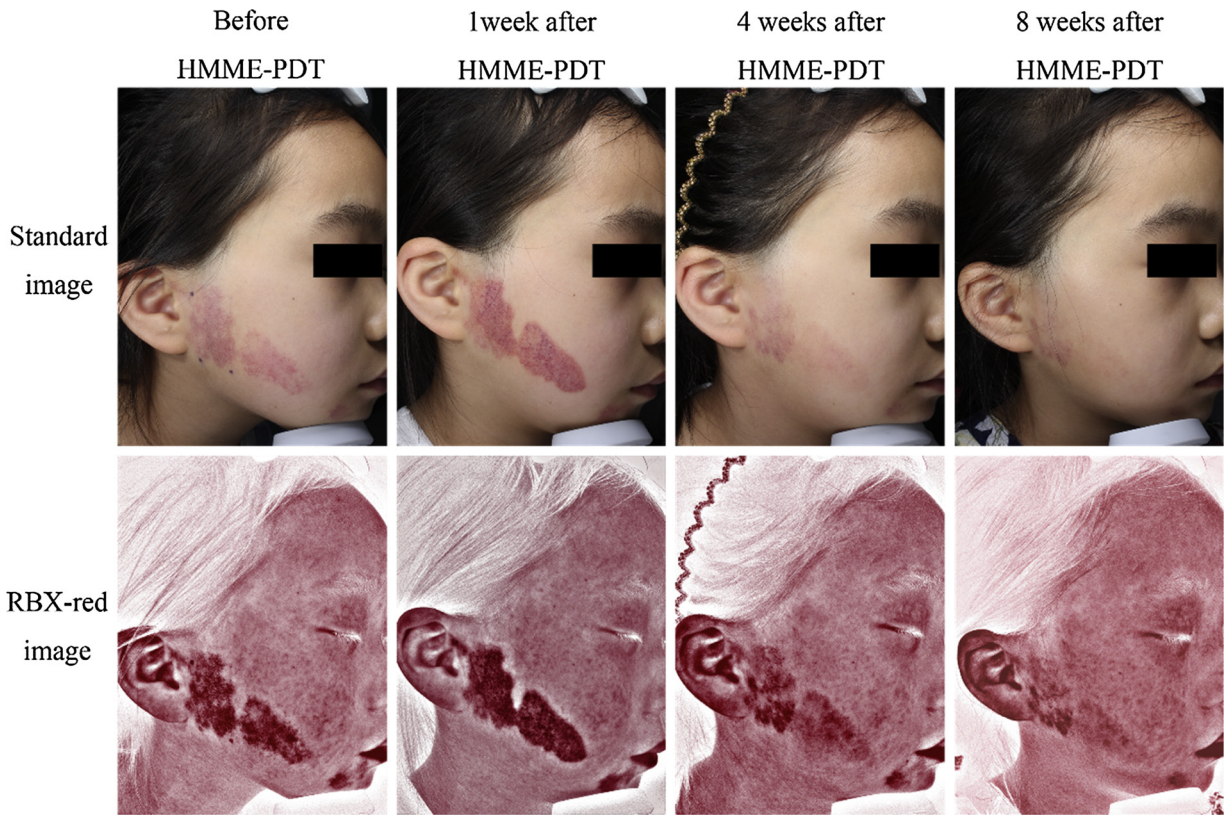

Fig. 2. Typical case of PWS patient treated by HMME-PDT detected by VISIA-CR™ system at different time points. The VISIA standard image shows the color fading in the lesion before and after HMME-PDT; RBX red image shows that the blood vessels in the lesion of PWS patients are highly aggregated and densely distributed, and the color of the lesion is deepened after PDT treatment and one week after treatment. Subsequently, the color of the lesion subsided gradually from 4 to 8 weeks.

diseased blood vessel. It reflected the suitability of the therapeutic dose and dose selection. In addition, the erythema index can be obtained by the analysis system. The degree of regression of the erythema index basically correlated with the efficacy grading. Moreover, the erythema index reduced value *d* during the follow-up can reflect the curative effect. Further, the erythema index can assist in curative effect evaluation. The efficacy evaluation through the VISIA-CR™ system's RBX red image showed higher response rate than the visual evaluation. The VISIA-CR™ system's RBX red image more sensitively reflects color blanching of baseline in the treated area.

4.2. The application value of dermoscopy

The application of dermoscopy in PWS has also been reported previously [26–29]. Most studies evaluated the changes in skin lesions after PDL treatment. However, there was no report on the application of

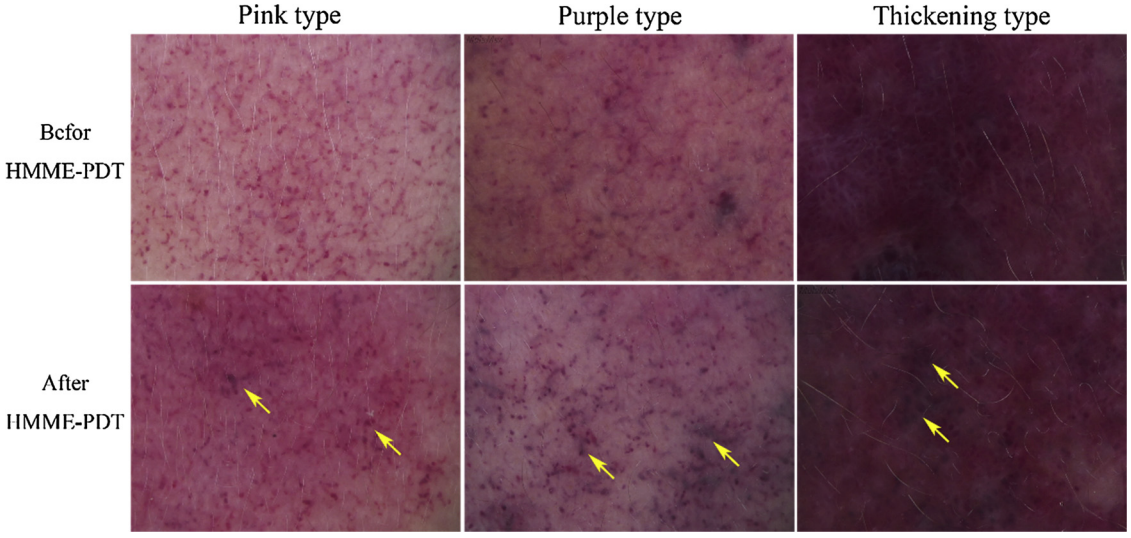

Fig. 3. Dermoscopy for different type of PWS with HMME-PDT. The pink type showed irregular linear and spot-like blood vessels on a bright red background; the purple type showed a densely distributed spherical blood vessel on the deep red background; the thickening type showed lump-like blood vessels on the magenta background. After the treatment with HMME-PDT, the signs of vascular rupture (yellow arrows) were observed.

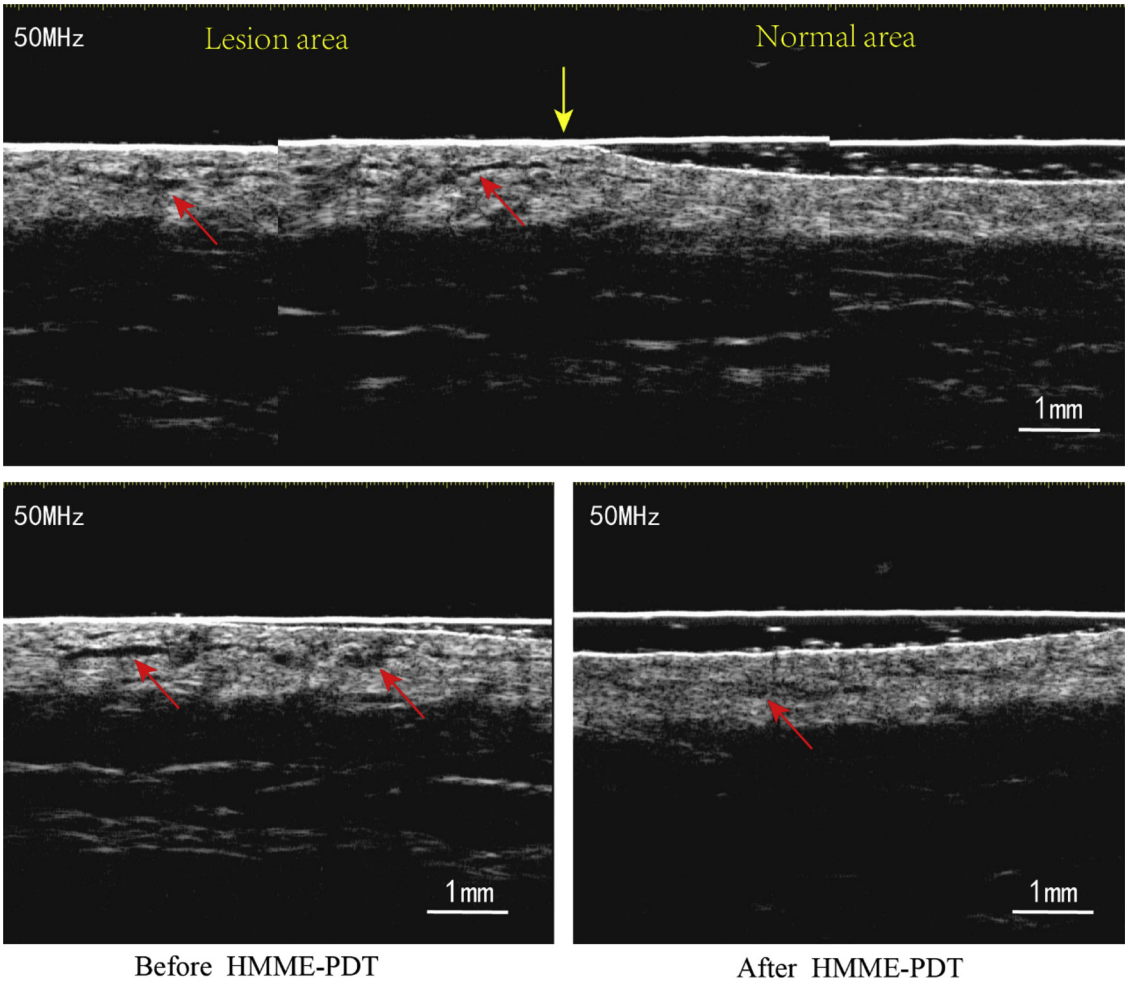

Fig. 4. Typical case of High-frequency ultrasound for PWS patient with HMME-PDT. HFUS showed that the skin lesions were more skin thickness than the normal skin, and the dermis was loosely arranged. After HMME-PDT, the thickened dermis was significantly thinner and the linear hypoechoic signal was significantly reduced and denser in all groups than in the treatment before treatment, which was more similar to that of normal skin. (Red arrows: blood vessels in the dermis; yellow arrows: boundaries between the erythema area and normal skin).

HMME-PDT in the evaluation of curative effect. Some interesting phenomena had been observed in this study.

The results showed that different types of PWS had various manifestations under dermoscopy, as shown in the results. Some studies reported that the lesions of the spherical blood vessels were mostly superficial, and the lesions of the linear blood vessels were deep [30], which were consistent with our results. After HMME-PDT, the lesions showed vascular rupture, punctate, or globular hemorrhagic shadows. Late observations showed that skin lesions with vascular rupture had better effect. This phenomenon might be a predictive marker of the curative effect. Simultaneously, the phenomenon of vascular rupture could be used as the end point of treatment to avoid other side effects. In addition, dermoscopy can display the shape and distribution of diseased blood vessels after treatment and provided an objective basis for HMME-PDT effect.

4.3. The application value of HFUS

The lesions in PWS were mainly located in the papillary and reticular layers of the dermis. The mean depths of the PWS vessels were 0.510 mm in the central sites and 0.289 mm in the lateral sites of the face [31]. The HMME-PDT light source is 532-nm LED light, which can penetrate the superficial layer of the dermis [32]. The previous study showed that the prognosis of PWS was related to the thickness and depth of the vessel. It was important to evaluate the thickness of PWS before HMME-PDT. It was necessary to evaluate the above factors objectively and accurately. Therefore, in this study, 20–50-MHz HFUS with a penetration depth of 4–10 mm was used to detect lesions in PWS and surrounding normal skin before and after HMME-PDT.

In this study, it was observed that the lesions were significantly thicker than the normal skin, the dermis was arranged loosely, and there was a linear hypoechoic signal. The linear hypoechoic signal was considered to be a significantly dilated or deformed blood vessel. Lesions in PWS without linear hypoechoic signal in the dermis showed better efficacy after HMME-PDT ($P < 0.05$). The linear hypoechoic signal might be used as an indicator of prognosis. However, not all skin lesions had this ultrasonographic feature. It might be because most PWS blood vessels were shallow and small in diameter, and the resolution of the existing HFUS cannot respond to its blood vessels. After HMME-PDT, it was observed that, in patients with good curative effect, the thickness of skin lesions decreased markedly, linear hypoechoic signal decreased, and tissue tended to compact. PDT may have targeted vascular endothelial cells to close the blood vessels and normalize the skin tissue. It can be inferred that the application prospect of HFUS in HMME-PDT depends on the improvement of US frequency.

4.4. The application value of LSCI

LSCI showed that lesions in PWS showed a rich perfusion signal compared with the normal skin. It was found that some lesions after

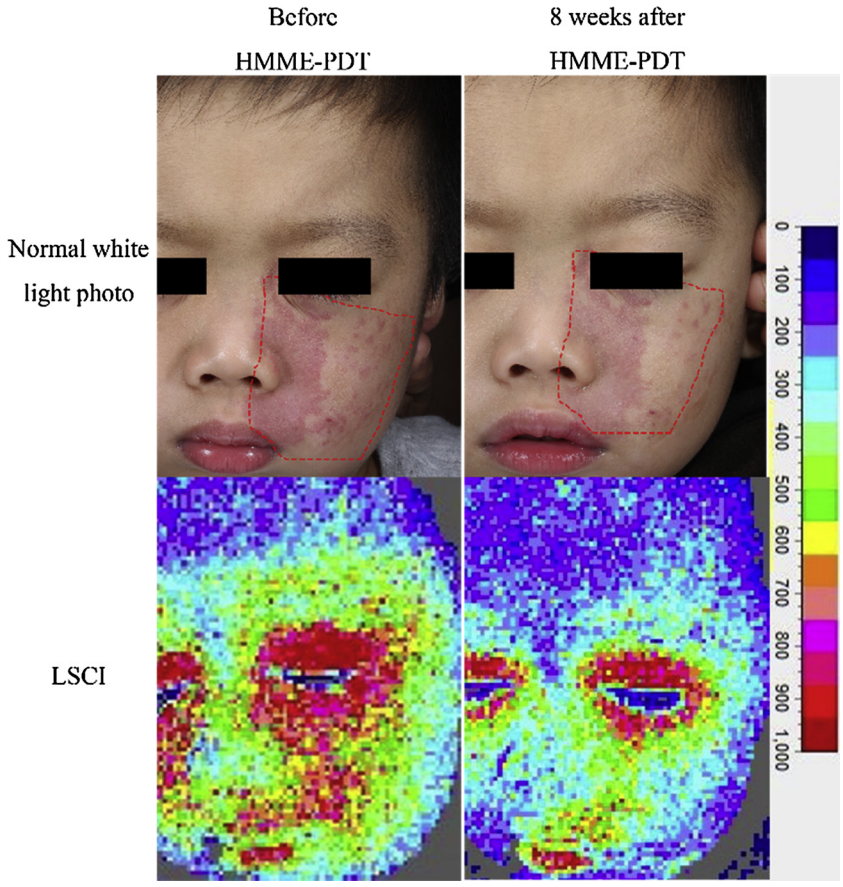

Fig. 5. Typical case of laser speckle contrast imaging for PWS patient with HMME-PDT. Erythema in treatment area subsided obviously, and LSCI showed that blood perfusion signal was significantly reduced.

PDT showed a decrease in blood perfusion, while some effective lesions did not show blood perfusion reduction. The possible reason for this phenomenon is that LSCI can detect the reduction of inconspicuous local perfusion. Accumulated blood after local vascular rupture is not completely absorbed, resulting in unsatisfactory bleaching of lesions. We found that most lesions had further bleaching even without further treatment. In addition, skin blood perfusion may be affected by several factors, such as environmental temperature and physical activity [33]. Therefore, LSCI measurement needs to be performed in a temperature-controlled room, and the patient needs a certain adaptation period before measurement and, during the measurement period, needs to remain stationary. It requires higher degree of patient compliance. Therefore, it was impossible to detect children with or without mental illness. This was the limitation of the method.

5. Conclusion

Invisible lesions can be observed using the VISIA-CR™ system before treatment. Moreover, lesions fading after HMME-PDT can be described objectively by this system. Dermoscopy plays an important role in the clinical classification of PWS, assessing vascular injury after HMME-PDT, guiding the adjustment of therapeutic dose, and selecting the end point of treatment. The thickness of PWS and depth of deformed blood vessels can be determined by HFUS. LSCI can be used to detect changes in blood perfusion of PWS lesions after HMME-PDT. HFUS and LSCI can assist in the evaluation of HMME-PDT response.

Acknowledgements

This study was supported by National Key Research and Development Program of China (2017YFC0111405), National Natural Science Youth Fund Project (81803156), Shanghai Science and Technology Committee (STCSM) (17411952500), Talent youth program of Shanghai Health and Family planning system (2017YQ066) and Shanghai Pujiang Program (17PJ1408500).

References

[1] B. Tallman, O.T. Tan, J.G. Morelli, J. Piepenbrink, T.J. Stafford, S. Trainor, et al., Location of port-wine stains and the likelihood of ophthalmic and/or central nervous system complications, Pediatrics 87 (1991) 323–327.
[2] J.K. Chen, P. Ghasri, G. Aguilar, A.M. van Drooge, A. Wolkerstorfer, K.M. Kelly, et al., An overview of clinical and experimental treatment modalities for port wine stains, J. Am. Acad. Dermatol. 67 (2012) 289–304.
[3] Y. Zhao, P. Tu, G. Zhou, Z. Zhou, X. Lin, H. Yang, et al., Hemoporfin photodynamic therapy for port-wine stain: a randomized controlled trial, PLoS One 11 (2016) e156219.
[4] R. Demirli, P. Otto, R. Vishwanathan, RBX® technology overview, Canfield Systems White Paper, (2007).
[5] A. Goldsberry, C.W. Hanke, K.E. Hanke, VISIA system: a possible tool in the cosmetic practice, J. Drugs Dermatol. 13 (2014) 1312.
[6] A. Blum, J. Kreusch, W. Stolz, H. Haenssle, R. Braun, R. Hofmann-Wellenhof, et al., Dermoscopy for malignant and benign skin tumors: indication and standardized terminology, Hautarzt 68 (2017) 653–673.
[7] G. Argenziano, H.P. Soyer, Dermoscopy of pigmented skin lesions–a valuable tool for early diagnosis of melanoma, Lancet Oncol. 2 (2001) 443–449.
[8] M.A. Pizzichetta, H. Kittler, I. Stanganelli, R. Bono, S. Cavicchini, V. De Giorgi, et al., Pigmented nodular melanoma: the predictive value of dermoscopic features using multivariate analysis, Br. J. Dermatol. 173 (2015) 106–114.
[9] H. Alexander, D.L. Miller, Determining skin thickness with pulsed ultra sound, J. Invest. Dermatol. 72 (1979) 17–19.
[10] F. Alfageme Roldán, Ecografía cutánea, Actas Dermo-Sifiliográficas 105 (2014) 891–899.
[11] K.R. Volz, C.D. Kanner, J. Evans, K.D. Evans, Klippel-trenaunay syndrome: need for careful clinical classification, J. Ultrasound Med. 35 (2016) 2057–2065.
[12] J.D. Briers, Laser Doppler, speckle and related techniques for blood perfusion mapping and imaging, Physiol. Meas. 22 (2001) R35–66.

[13] S. Eriksson, J. Nilsson, G. Lindell, C. Sturesson, Laser speckle contrast imaging for intraoperative assessment of liver microcirculation: a clinical pilot study, Med. Devices (Auckl.) 7 (2014) 257–261.
[14] N. Hecht, J. Woitzik, S. Konig, P. Horn, P. Vajkoczy, Laser speckle imaging allows real-time intraoperative blood flow assessment during neurosurgical procedures, J. Cereb. Blood Flow Metab. 33 (2013) 1000–1007.
[15] E. Klijn, H.C. Hulscher, R.K. Balvers, W.P.J. Holland, J. Bakker, A.J.P.E. Vincent, et al., Laser speckle imaging identification of increases in cortical microcirculatory blood flow induced by motor activity during awake craniotomy, J. Neurosurg. 118 (2013) 280.
[16] R. Bezemer, M. Legrand, E. Klijn, M. Heger, I.C. Post, T.M. van Gulik, et al., Real-time assessment of renal cortical microvascular perfusion heterogeneities using near-infrared laser speckle imaging, Opt. Express 18 (2010) 15054–15061.
[17] C. Sturesson, D.M. Milstein, I.C. Post, A.M. Maas, T.M. van Gulik, Laser speckle contrast imaging for assessment of liver microcirculation, Microvasc. Res. 87 (2013) 34–40.
[18] Y. Zhang, X. Zou, H. Chen, Y. Yang, H. Lin, X. Guo, Clinical study on clinical operation and post-treatment reactions of HMME-PDT in treatment of PWS, Photodiagn. Photodyn. Ther. 20 (2017) 253–256.
[19] K. Minkis, R.G. Geronemus, E.K. Hale, Port wine stain progression: a potential consequence of delayed and inadequate treatment? Lasers Surg. Med. 41 (2009) 423–426.
[20] S.W. Lanigan, S.M. Taibjee, Recent advances in laser treatment of port-wine stains, Br. J. Dermatol. 151 (2004) 527–533.
[21] R. Anolik, T. Newlove, E.T. Weiss, L. Brightman, E.K. Hale, J.K. Karen, et al., Investigation into optimal treatment intervals of facial port-wine stains using the pulsed dye laser, J. Am. Acad. Dermatol. 67 (2012) 985–990.
[22] K. Reddy, L. Brightman, R. Geronemus, Laser treatment of port-wine stains, Clin. Cosmet. Investig. Dermatol. 8 (2015) 27.
[23] Y. Tang, H. Xie, J. Li, D. Jian, The association between treatment reactions and treatment efficiency of HMME-photodynamic therapy on port wine stains: a prospective double blind randomized controlled trial, Photodiagn. Photodyn. Ther. 18 (2017) 171–178.
[24] S.A. Sharif, E. Taydas, A. Mazhar, R. Rahimian, K.M. Kelly, B. Choi, et al., Noninvasive clinical assessment of port-wine stain birthmarks using current and future optical imaging technology: a review, Br. J. Dermatol. 167 (2012) 1215–1223.
[25] G. Micali, F. Dall Oglio, A.E. Verzì, I. Luppino, K. Bhatt, F. Lacarrubba, Treatment of erythemato-telangiectatic rosacea with brimonidine alone or combined with vascular laser based on preliminary instrumental evaluation of the vascular component, Laser Med. Sci. 33 (2017) 1397–1400.
[26] A. Sevila, E. Nagore, R. Botella-Estrada, O. Sanmartin, C. Requena, C. Serra-Guillen, et al., Videomicroscopy of venular malformations (port-wine stain type): prediction of response to pulsed dye laser, Pediatr. Dermatol. 21 (2004) 589–596.
[27] M.A. Al-Dhalimi, M.H. Al-Janabi, Split lesion randomized comparative study between long pulsed Nd:YAG laser 532 and 1,064 nm in treatment of facial port-wine stain, Lasers Surg. Med. 48 (2016) 852–858.
[28] R. Moriuchi, K. Kikuchi, T. Ito, S. Shimizu, Acquired plantar port-wine stain showing a red parallel ridge pattern under dermoscopy, Clin. Exp. Dermatol. 39 (2014) 944–945.
[29] M. Shirakawa, T. Ozawa, S. Wakami, M. Ishii, T. Harada, Utility of dermoscopy before and after laser irradiation in port wine stains, Ann. Dermatol. 24 (2012) 7.
[30] S. Kwon, Y. Yoon, B. Kim, W.H. Jang, B. Oh, K.Y. Chung, et al., Dermoscopy guided dark-field multi-functional optical coherence tomography, Biomed. Opt. Express 8 (2017) 1372.
[31] W. Yu, G. Ma, Y. Qiu, H. Chen, Y. Jin, X. Yang, et al., Why do port-wine stains (PWS) on the lateral face respond better to pulsed dye laser (PDL) than those located on the central face? J. Am. Acad. Dermatol. 74 (2016) 527–535.
[32] Y. Pu, W. Chen, Z. Yu, Research progress of Hemoporfin–part one: preclinical study, Photodiagn. Photodyn. Ther. 9 (2012) 180–185.
[33] D.J. McGill, I.R. Mackay, The effect of ambient temperature on capillary vascular malformations, Br. J. Dermatol. 154 (2006) 896–903.